Water Air Soil Pollut (2024) 235:465
https://doi.org/10.1007/s11270-024-07271-6

Carbon, Nitrogen, and Phosphorus Fluxes in Sixty Tropical Brazilian Rivers: Current Status, Stoichiometry and Trends

Carlos Noriega · Humberto Varona · Carmen Medeiros · Aubains Hounsou-Gbo · Julia Araujo · Moacyr Araujo

Received: 5 December 2023 / Accepted: 13 June 2024 / Published online: 25 June 2024

Abstract Public data from sixty tropical rivers were used to explore variations in C, N, and P and the potential impact of anthropogenic activities over a decade on freshwater bodies. The results showed the Total Organic Carbon (TOC) varying between 2.7–73.0 mg C l^{-1}; whereas Total Nitrogen observations showed concentrations between 0.9 and 32.0 mg N l^{-1} and Total Phosphorus showed a higher frequency of data in the range of 0.02–0.4 mg P l^{-1}. The annual total C load (TC) was estimated at 32.7 Tg C yr^{-1}, where dissolved inorganic carbon (DIC) accounted for 69% of TC and dissolved organic carbon (DOC) contributed 22%. The stoichiometry showed P depletion relative to C and/or N in 39 of the sixty rivers (65%). This was further supported by the fact that most catchments had TOC values > 50% (C/N/P = 100%). A significant trend was found for yearly fluxes of TOC for the period 2008–2018 (Mann–Kendall test; $p = 0.0006$; $\alpha = 0.05$). Land-use and cover at period 2008–2018 indicated a trend of increasing anthropized area of 4%, whereas the natural area decreased by 3.1%. The organic load trend analysis showed 85% of municipalities with a positive trend, this high rate in the remaining organic load is indicative of urban and agricultural in the region.

Keywords Tropical Rivers · Carbon · Nitrogen · Phosphorus · Fluxes · Stoichiometry

1 Introduction

Riverine supply of many elements, including carbon, nitrogen and phosphorus of largely terrestrial origin, is important to the steady-state chemistry of the oceans (Wachholz et al., 2023; Bauer et al., 2013). Metabolism in temperate coastal systems is associated with the magnitude of nutrient loads (carbon-C, nitrogen-N, and phosphorus-P) derived from the Earth to the Ocean (Wachholz et al., 2023; Tanioka et al., 2022; Liu et al., 2020; Causse et al., 2015; Eyre & Ferguson, 2002); however, in tropical systems, there are still uncertainties about the impact that these loads generate in the coastal region. Some authors indicate that this is mainly due to the interaction of multiple physical and biogeochemical

Supplementary Information The online version contains supplementary material available at https://doi.org/10.1007/s11270-024-07271-6.

C. Noriega (✉) · H. Varona · C. Medeiros · J. Araujo · M. Araujo
Department of Oceanography, Federal University of Pernambuco, Recife, Brazil
e-mail: cnoriega.ufpe@gmail.com

C. Noriega · H. Varona · M. Araujo
Center for Risk Analysis, Reliability Engineering and Environmental Modeling (CEERMA), Federal University of Pernambuco, Recife, PE, Brazil

A. Hounsou-Gbo
LABOMAR- Federal University of Ceará, Av. da Abolição, Fortaleza 3207, Brazil

factors (Causse et al., 2015; Jani & Toor, 2018; Eyre & Ferguson, 2002). Riverine nutrient loading, C, N, and P, is increasing in many catchments worldwide due to changes in land management, farming practices, and increasing urbanization (Gruber and Galloway, 2008; Blaen et al., 2017).

These changes are mainly intensified by the increase in land use cover and the increase in the population density rate that provides high rates of remaining organic load to rivers mainly in cities with low percentage of sewage treatment. These changes may also alter the rates of C, N, and P available for aquatic metabolism in tropical rivers.

According to Peacock et al. (2022), ecosystems and processes are dynamically linked through the transfer of water, solutes, and particles from the headwaters to the sea, and by interactions between different elements in biogeochemical cycles, particularly C, N, and P. Consequently, changes in the ecological status and management of terrestrial systems have the potential to alter the condition and function of downstream coastal and freshwater ecosystems, and the goods and services they provide, in ways that cannot be easily predicted from the study of single systems or individual processes. Several studies in the last decade have suggested that element ratios (stoichiometry) may provide a more effective indicator of ecosystem status than individual nutrient concentrations (Jarvie et al., 2018; Peacock et al., 2022; Stutter et al., 2018; Wachholz et al., 2023). According to Islam et al. (2019), changes in the stoichiometry of organic matter are associated with nutrient cycling and ecosystem biogeochemical processes. Thus, the transformations of N and P in organic forms reflect the assimilation and dissimilation of these important nutrients. Organic matter is initially synthesized in aquatic ecosystems mostly through algal photosynthesis and microbial activity, and the C:N:P ratio is well known to be close to the Redfield ratio (106:16:1). However, during the decomposition of organic matter, the behavior and the rates of mineralization of C, N, and P can vary. It is known that the mineralization rate of organic P is much faster than the mineralization rate of organic C and N, resulting in the deviation of C:N:P ratio from the Redfield ratio (Islam et al., 2019; Jeanneau et al., 2018). Another factor that affects C:N:P ratio of organic matter in rivers is the input of allochthones organic matter via wastewater, livestock, agriculture, etc.

The study region includes large coastal cities with high population density rates and regions of high agricultural activity in inland municipalities. In this paper, we explore the hypothesis that, globally, the stoichiometric proportions of C, N, and P are altered as agriculture and urbanization intensify. In doing so, we aim to make connections between increases in these elements (fluxes and concentrations) in sources of input and changes in nature. We used public data from sixty tropical rivers (drainage area: 20 km^2 to 6.6×10^5 km^2) to explore variations in C, N, and P and the potential impact of anthropogenic activities over a decade on freshwater bodies.

2 Methods

2.1 Study Area

The study region has an estimated area of 564,760 km^2 which represents 6.7% of the area of the Brazilian territory. This region corresponds to the state of Bahia with a population of 14,930,634 million people, a demographic density of 24.8 inhab km^{-2}, and is divided into 417 municipalities (IBGE, 2010). The hydrographic network of the region covers the geographic coordinates -46.6 to -37.3ºW longitude and -18.3 to -8.5ºS latitude. This region includes two of the seven major Brazilian hydrographic regions (Eastern Atlantic and São Francisco) with a drainage area of 1,014,667 km^2. This region also includes major river basins such as São Francisco, Contas, Paraguaçu, Itapecuru, Grande, and Jequitinhonha (Fig. 1 and Table 1), with a strong amplitude between drainage areas (between 20 km^2 and 600,000 km^2). Through this hydrographic network, 453 fluviometric stations measure flows and limnimetric quotas, administered by governmental entities such as ANA (National Water Agency), CODEVASF (São Francisco Valley Development Company), CRA (Regional Administration Council of the State of Bahia), and INGÁ (Water Management Institute). Mean river discharges in the region vary strongly from small streams (< 1.0 m^3 s^{-1}) to large rivers ($> 1{,}000$ m^3 s^{-1}).

Another network managed by INMET (National Institute of Meteorology) collects meteorological data through 29 stations in this region. This network shows an amplitude of rainfall in the region that oscillates between 400 and 1300 mm per year (INMET,

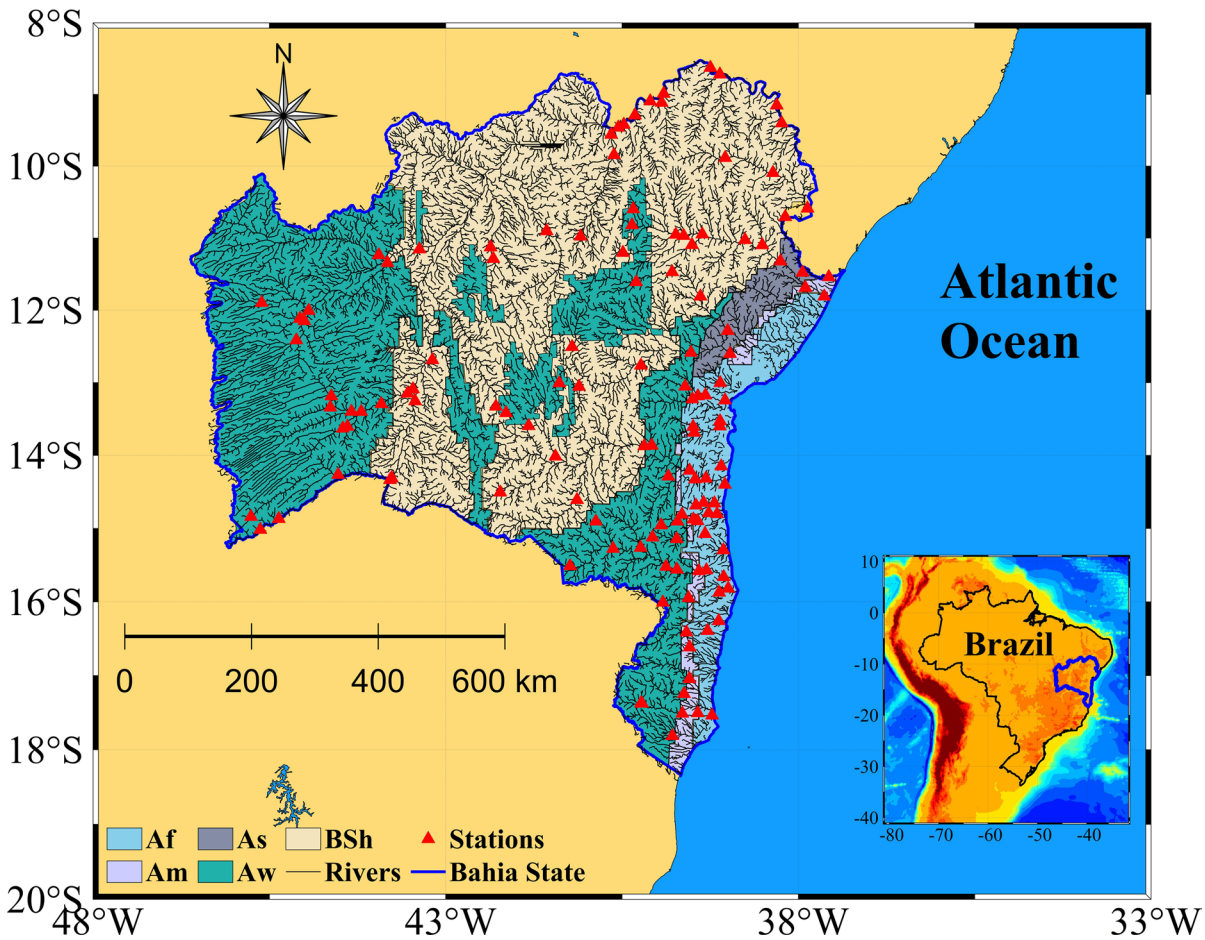

Fig. 1 Study region (blue polygon) and hydrographic network (gray polygon) including monitoring stations (red triangles). The colors in the study region correspond to the Koppen climate classification

2018). Additionally, water quality data were collected at 143 stations by INEMA (Institute of Environment and Water Resources) throughout the Bahia-Brazil state region (INEMA, 2018). These parameters are indicated in Table 2.

In the northeast region of Brazil, there are five climatic types according to the Köppen climate classification (Noriega & Araujo, 2014). The climatic types present in the study region are Af, Am, As, Aw, and BSh. These range from humid equatorial climates (tropical rainforests) to semi-arid types (Fig. 1). According to EMBRAPA (Empresa Brasileira de Pesquisa Agropecuária) estimates from Santos et al (2018) publications, the soils that prevail in the region are latosoils, argisoils, and neosoils, representing ~ 70% of the total (Fig. 1S).

2.2 Data Sources

Data on physical and chemical parameters were obtained bimonthly by INEMA (www.inema.ba.gov.br) for the period 2008–2018 and analyzed for Total Organic Carbon (TOC), Total Dissolved Nitrogen (DIN), Total Nitrogen (TN), Total Dissolved Phosphorus (DIP), Total P (TP) and Total Alkalinity (TA). Dissolved Inorganic C (DIC) was calculated from pH, alkalinity, and water temperature measurements using the mStatGraph v1.7 software (Varona et al., 2023). Total carbon (TC) was calculated as the sum of TOC and DIC. The organic particulate forms of C (POC), N (PON), and P (POP), were obtained through the differences between the dissolved and total forms. Additionally, rainfall data were obtained

Table 1 General characteristics of watersheds. Climate types are represented in Fig. 1. All data refer to the period 2008–2018

River [code]	Drainage area (km^2)	Discharge (average) ($m^3\ s^{-1}$)	Climate Types (Köppen)	Population density (inhab km^2)	Rainfall (average) (mm)
Almada [ALM]	1575	9.4	Af	190	1000
Colonia [COL]	1414	2.3	Aw	77	730
Cachoeira [RCH]	4330	24.1	Af	138	1006
Salgado [SLD]	1020	2.2	Aw, Af	48	613
Salomé [SLM]	60	0.6	Af	30	700
Una [UNA]	1790	13.2	Af	13	1100
Tijuípe [TIJ]	75	0.7	Af	30	1200
Das Almas [DAL]	2380	14.5	Af	35	900
Baiano [BAI]	183	1	Af	12	1200
Camarugi [CMG]	168	0.8	Af	25	1300
Jaguaripe [JGP]	2200	5.0	Af	60	1000
Jequiriçá mirim [JQM]	1560	15	Aw	20	800
Jequiriçá [JQR]	7000	5.2	Af	29	1060
Preto [P13]	1080	7	Af	22	800
Carinhanha [CRN]	17000	146	Aw, BSh	4	720
Itaguari [IGR]	6500	40	Aw	3	575
Corrente [CRT]	35000	27.7	Aw, BSh	4	654
Formoso [FOM]	9945	39.5	Aw	2	500
Guará [GUA]	13700	7.4	Aw	3	850
Do Antonio [ANT]	5187	6.7	BSh	10	830
Brumado [BRU]	284	1	BSh	15	400
Contas [COM]	55200	23	BSh, Aw, Af	20	740
Gavião [GAV]	11000	1	BSh	15	500
Gongoji [GGI]	5800	10	Af	26	1000
Jequiezinho [JQZ]	1340	10	Aw	120	600
Do Peixe [PEX]	377	1.3	Aw	39	850
Das Femeas [FEM]	6472	32	Aw	5	780
Grande [GRD]	77967	104	Aw, BSh	6	850
Preto [P11]	22250	49	Aw	3	900
Branco [RBR]	8230	55	Aw	3	850
De Janeiro [RJN]	3296	13	Aw	18	700
De Ondas [RON]	5590	17	Aw	30	800
Do Aipim [AIP]	904	17.2	Aw	39	700
Itapicuru açu [ITA]	2850	3	Aw	30	600
Itapicuru [ITP]	36900	38	BSh, Am, Af	27	690
Peixe de baixo [RPB]	1508	13	BSh	20	420
Itapicuru mirim [ITM]	3550	3	BSh	22	600
Jequitinhonha [JQH]	70920	144	Aw, Af	11	930
Jacuípe [JCP]	11935	1	BSh, As	49	530
Paraguaçu [PRG]	55383	25	Aw, BSh, Am	20	660
De Una [RDU]	1797	5	BSh	60	500
Utinga [UTG]	2760	2	BSh	15	800
Catolé Grande [CGR]	3107	9	Aw	30	560
Córrego Lagoa do Baixo [CLB]	20	0.5	Aw	90	600

Table 1 (continued)

River [code]	Drainage area (km^2)	Discharge (average) ($m^3\ s^{-1}$)	Climate Types (Köppen)	Population density (inhab km^2)	Rainfall (average) (mm)
Pardo [PRD]	32152	17	Aw, Am, Af	22	750
Real [REA]	4713	5	BSh, As, Am	5	860
Salitre [SAL]	14490	8	BSh	11	420
Vaza-Barris [VZB]	14123	56	BSh, As	24	503
Buranhém [BRH]	2700	20	Am, Af	50	1050
Dos Frades [FRD]	828	9	Am	36	1000
São Francisco [RSF]	616100	1654	BSh	8	400
João de Tiba [JTB]	1580	20	Af	80	1000
Curaçá [CRC]	3773	6	BSh	8	500
Paramirim [PMI]	17410	15	BSh	4	510
Alcobaça [ALB]	6554	25	Aw, Am, Af	29	1030
Jucuruçu Braço Norte [JUN]	2834	18	Am	22	950
Jucuruçu Braço Sul [JUS]	2198	14	Aw	8	980
Peruípe do Sul [PRP]	1423	10	Aw	10	1200
Jacaré [JRE]	15800	1	BSh	5	480
Verde [VRD]	30420	75	BSh	2	500

Table 2 Analytical methodologies of the variables used in the monitoring for the period 2008–2018

Parameter [units]	Analytical methodology	References
Total Alkalinity [mg l^{-1}]	Standard Methods (SM 2320 A/B)	APHA (2005) Standard Methods for the Examination of Water and Wastewater. 21st Edition, American Public Health Association/ American Water Works Association/Water Environment Federation, Washington DC
Temperature [ºC]	Standard Methods (SM 2550 B)	
pH	Standard Methods (SM 4500 H + B)	
Total Nitrogen [mg l^{-1}]	Standard Methods (4500-N)	
Dissolved Inorganic Phosphorus [mg l^{-1}]	4500-P B. Ascorbic Acid Method	
Total Phosphorus [mg l^{-1}]	Standard Methods (SM 4500 P)	
Total Organic Carbon [mg l^{-1}]	Standard Methods (SM 5310)	

from INMET (www.inmet.gov.br) for the same study period. River discharge records were obtained from ANA (www.ana.gov.br). Demographic data (population density) were obtained from the IBGE (www.ibge.gov.br) and associated with the watersheds and corresponding municipalities. The spatial distribution of mineral resources (limestone, silica, and sedimentary) was obtained from the updated GLORICH database. The analysis methodologies of the physical–chemical parameters are shown in Table 2.

Total Alkalinity [mg l^{-1}], as $CaCO_3$ by titration method was used to measure the total alkalinity of water, which is the water's ability to neutralize acids. The precision of this method is ± 0.1 mg l^{-1} for samples with total alkalinity of up to 100 mg l^{-1} and ± 0.2 mg l^{-1} for samples with total alkalinity greater than 100 mg l^{-1}. Samples were sampling in polyethylene bottles and store at a low temperature.

Temperature [ºC]: the precision of this method is ± 0.1 ºC for samples with temperatures up to 40 ºC and ± 0.2 ºC for samples with temperatures greater than 40 ºC. pH: the precision of this method is ± 0.02 pH units for samples with pH up to 7.0 and ± 0.03 pH units for samples with pH greater than 7.0. Total Nitrogen [mg l^{-1}]—Method 4500-N: this method was used to measure the total nitrogen in water, which is the sum of all forms of nitrogen in water ($NO_3^- + NO_2^- + NH_4^+$). The precision of

this method is ± 0.2 mg l^{-1} for samples with total nitrogen up to 10 mg l^{-1} and ± 0.5 mg l^{-1} for samples with total nitrogen greater than 10 mg l^{-1}. Total nitrogen was determined through the oxidative digestion of all digestible nitrogen forms to nitrate, followed by quantitation of the nitrate using an in-line persulfate/UV digestion (4500-N/B) of Standard Methods.

Dissolved Inorganic Phosphorus [mg l^{-1}]: this method was used to measure the dissolved inorganic phosphorus in water, which is the form of phosphorus that is more readily available to phytoplankton's. The precision of this method is ± 0.05 mg l^{-1} for samples with dissolved inorganic phosphorus up to 0.5 mg l^{-1} and ± 0.1 mg l^{-1} for samples with dissolved inorganic phosphorus greater than 0.5 mg l^{-1}.

Total Phosphorus [mg l^{-1}]: this method was used to measure all forms of phosphorus in water. The precision of this method is ± 0.2 mg l^{-1} for samples with total phosphorus up to 10 mg l^{-1} and ± 0.5 mg l^{-1} for samples with total phosphorus greater than 10 mg l^{-1}.

Total Organic Carbon [mg l^{-1}]: this method is used to measure the total organic carbon in water, which is the sum of all the organic carbon in water (DOC and POC). The precision of this method is ± 0.5 mg l^{-1} for samples with total organic carbon up to 100 mg l^{-1} and ± 1 mg l^{-1} for samples with total organic carbon greater than 100 mg l^{-1}. The sample is acidified, purged to remove inorganic carbon, and oxidized with persulfate in an autoclave at temperatures from 116 to 130 ºC. The resultant carbon dioxide (CO_2) is measured by nondispersive infrared spectrometry.

The sampling frequency of water samples for the analysis of physical and chemical parameters was bimonthly for each monitored station between 2008 and 2018. All samples were collected at the surface of each water body (< 1 m).

The weighted average element/compound concentration was calculated by the following equation:

$$Ci = \frac{\sum_{i=1}^{n} Cith * Qith}{\sum_{i=1}^{n} Qith} \quad (1)$$

where Ci is the weighted average element/compound concentration [mg l^{-1}], Ci, is the concentration for the ^{ith} measurement [mg l^{-1}] and Qi is the discharge of the river in the day of the *i*th measurement [m^3 s^{-1}]. The load of C, N and P for each sampling station was estimated from the expression: Load-CNP (tons per year) = Discharge (m^3 per year) × Concentration (g/m^3) / 1,000,000.

Descriptive Statistics The mean, standard deviation, minimum, maximum, and percentages were computed. Nonparametric statistics: the Mann–Whitney test was used to verify significant differences between two sample sets. The statistics for the time series were computed using the Mann–Kendall trend test. In the Mann–Kendall test, a trend is considered negative or positive, indicating a decrease or increase in the attributes of the historical series analyzed, if the Mann–Kendall (Kendall's tau) score is negative or positive, respectively. In addition, the trend indicated by this methodology is considered significant when the *p*-value has a value less than $\alpha = 0.05$. All statistical analyses were performed using mStatGraph v1.7 software (Varona et al., 2023).

3 Results

3.1 Rainfall and Fluvial Discharge

The analysis of rainfall for the period 2008–2018 did not show significant differences (Mann–Whitney; $p > 0.05$; $\alpha = 0.05$) with the historical period (30 years). Additionally, trend analysis (Mann–Kendall test) showed no statistically significant trend (Fig. 2S).

The rainfall regime of the coastal or coastal sector (E) and the rainfall regime of the interior region of the state of Bahia (W) were analyzed through a 30-year series (1960–2010) of data obtained from meteorological stations in the study region and we concluded that the wet period includes the months of April, May and June on the coast, and November, December, and January in the interior. The dry period includes the months of August, September, and October on the coast, and June, July, and August inland (Fig. 2S).

Fluvial discharges ranged from 0.5–1654 m^3 s^{-1} with maximum values observed in the São Francisco River. Other important river discharges were observed in the Carinhanha (146 m^3 s^{-1}), Jequitinhonha (144 m^3 s^{-1}) and Rio Grande (104 m^3 s^{-1}) rivers. The average value for the observed period was 49 m^3 s^{-1} for the 60 rivers studied (Table 1).

3.2 C-N-P Spatial Distribution of Observations

According to the observations of the period, TOC varied between 2.7–73.0 mg C l^{-1}, with an accumulation of values in the range of 10–20 mg C l^{-1} (Fig. 2a). The mean value of all sampling stations was 13.0 ± 10 mg C l^{-1}, while spatial averages showed maxima in the Peixe de Baixo, Salitre, Real, and Jequiezinho rivers. The lowest mean value was 2.7 mg C l^{-1}, observed in the Itaguari River (Table 1). The TA values observed over the period showed a wide range of values (1.80—372.0 mg TA l^{-1}); however, the highest frequency of data was concentrated in the 0–20 mg TA l^{-1} range (Fig. 3S). The mean value obtained for TA was 53.0 ± 66 mg TA l^{-1}. According to the spatial analysis, TA showed high mean values in the rivers Real (372.0 mg TA l^{-1}) and Jequiezinho (329.0 mg TA l^{-1}) respectively. Low values of TA were observed in the Paraguaçu (1.8 mg TA l^{-1}) and Formoso (2.7 mg TA l^{-1}) rivers, respectively (Table 1 and Fig. 2b). The observed inorganic/organic C ratio (TA/TOC) was 0.66 for all sampling stations.

TN observations showed concentrations between 0.9 and 32.0 mg N l^{-1} in the studied rivers. The highest frequency of data was concentrated in the range of 2–3 mg N l^{-1}, equivalent to 75% of the recorded observations (Figs. 2c and 3Sc). The mean value obtained for the 60 rivers was 2.5 ± 4 mg N l^{-1}; whereas the spatial means in the rivers showed a maximum mean of 32 mg N l^{-1} in Rio Real and a minimum mean of 0.9 mg N l^{-1} in Rio de Janeiro (Fig. 3Sc).

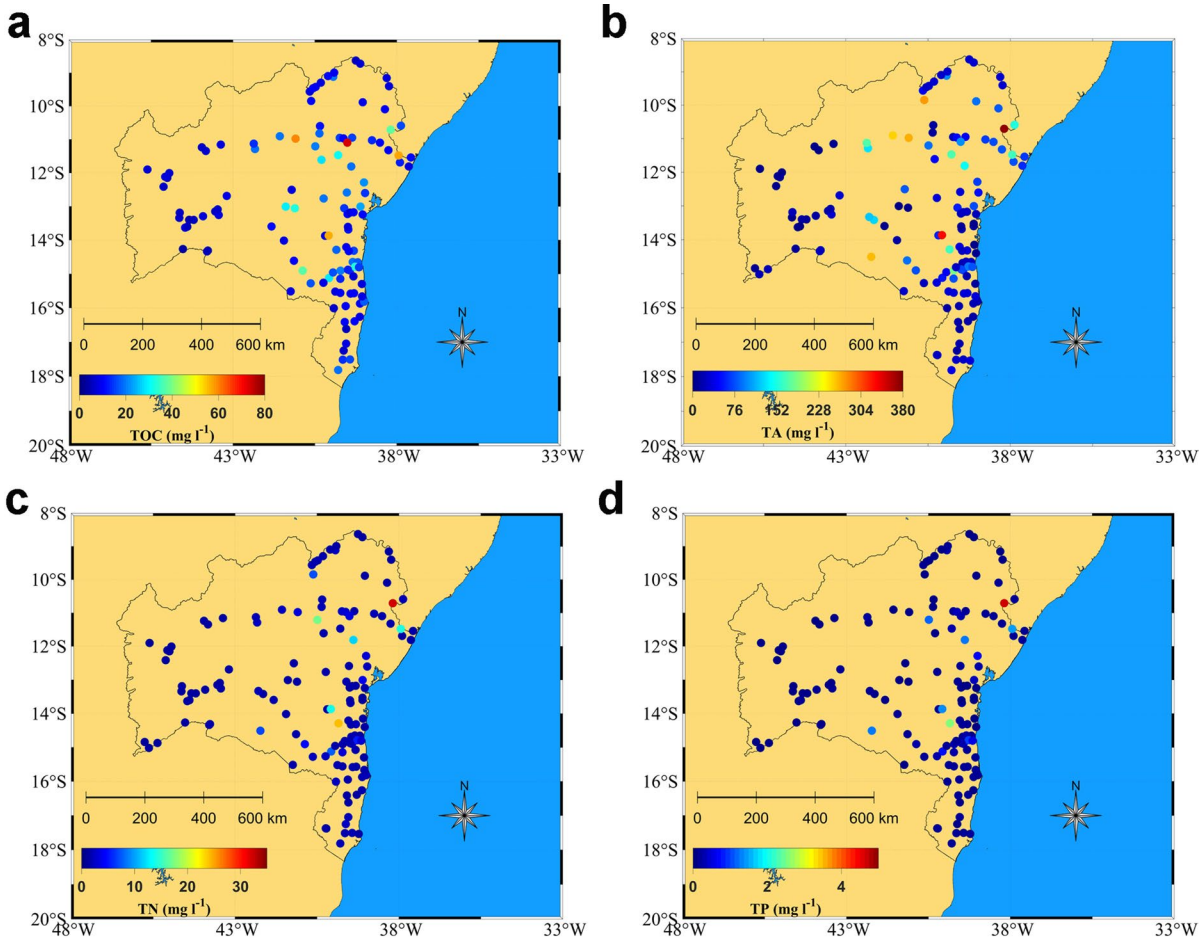

Fig. 2 Spatial distribution of the mean observed values per sampling station of TOC (**a**), TA (**b**), TN (**c**), and TP (**d**) in the studied rivers. The color bar indicates the concentration in mg $l.^{-1}$

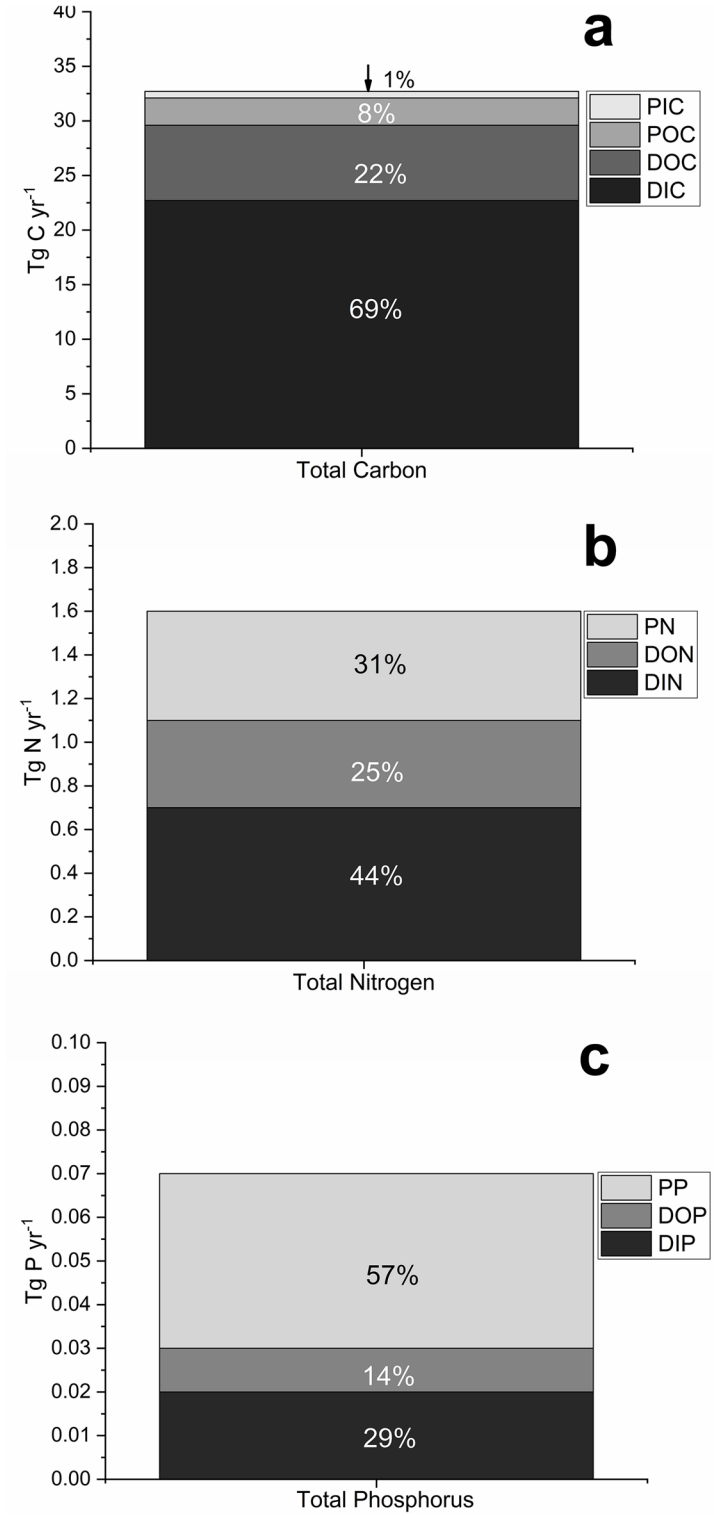

Fig. 3 C-N-P fluxes for the studied rivers between 2008 and 2018. **a** Carbon (Tg C yr^{-1}), **b** Nitrogen (Tg N yr^{-1}), and (**c**) Phosphorus (Tg P $yr.^{-1}$)

TP observations showed a mean concentration of 0.2 ± 0.5 mg P l^{-1} (Fig. 2d); while the histogram showed a higher frequency of data in the range of 0.0—0.4 mg P l^{-1}; however, values > 9 mg P l^{-1} were also recorded (Fig. 3Sd). The spatial averages showed a maximum average of 4.6 mg P l^{-1} in the Real River in the northern region of the state (Fig. 2d).

3.3 C-N-P Fluxes

Estimates of the C fluxes (Tg yr^{-1}) of the studied rivers are shown in Fig. 3a. The annual total C load (TC) was estimated at 32.7 Tg C yr^{-1} (0.0327 Pg C yr^{-1}), where DIC accounted for 69% of TC (22.7 Tg C yr^{-1}) and DOC contributed 22% (6.9 Tg C yr^{-1}), whereas particulate forms showed 8% for POC (2.50 Tg C yr^{-1}) and 1% for PIC (0.6 Tg C yr^{-1}). Estimated total N (TN) loads amounted to 1.6 Tg N yr^{-1} (Fig. 3b); distributed between DIN with 44% of TN (0.7 Tg N yr^{-1}), DON with 25% of TN (0.4 Tg N yr^{-1}), and PN with 31% (0.5 Tg N yr^{-1}) respectively.

P loads amounted to 0.07 Tg P yr^{-1} (Fig. 3c); where DIP accounted for 29% of the TP (0.02 Tg P yr^{-1}), DOP accounted for 14% of the total (0.01 Tg P yr^{-1}), and PP accounted for 57% of the TP (0.04 Tg P yr^{-1}) respectively.

3.4 C-N-P Trends

The observed yearly fluxes were estimated for TOC, TA, TN, and TP, indicating a statistically significant increment of TOC for the period 2008–2018 (Mann–Kendall test; $p = 0.0006$; $\alpha = 0.05$). The slope of this series indicated an increase of 0.001 g C m^{-2} yr^{-1} for the TOC time series (Fig. 4b). TA did not show a significant trend (Mann–Kendall

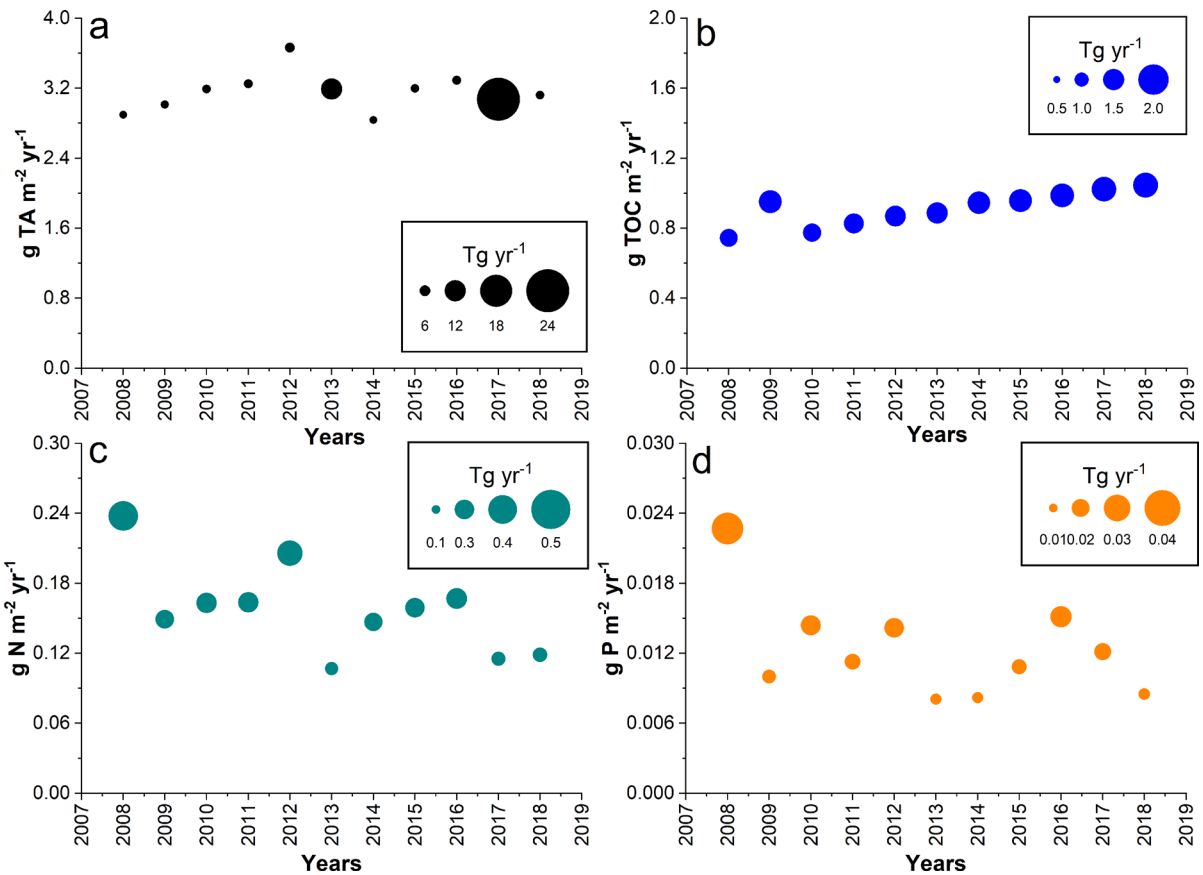

Fig. 4 Yearly fluxes (g m^{-2} yr^{-1}) of TA (**a**), TOC (**b**), TN (**c**), and TP (**d**), between 2008 and 2018 for the study region. The size of the bubbles refers to the annual loads (Tg yr^{-1}) for TA, TOC, TN and TP

test; $p > 0.05$; $\alpha = 0.05$); however, it recorded high loads (bubble size in Fig. 4a), especially in the years 2013 and 2017. TN and TP also showed no statistically significant trends (Mann–Kendall test; $p > 0.05$; $\alpha = 0.05$). The annual TN rate indicated a mean value of 0.03 ± 0.007 g N m^{-2} yr^{-1}; while TP showed a mean value of 0.02 ± 0.006 g P m^{-2} yr^{-1} (Fig. 4c and d). The mean annual TOC rate for the period indicated a value of 1.4 ± 0.15 g C m^{-2} yr^{-1}; whereas TA showed a lower mean annual rate than TOC (0.6 ± 0.04 g C m^{-2} yr^{-1}).

3.5 C-N-P Fluxes and Climate Types

The C-N-P fluxes for the climate types were grouped into five clusters (Fig. 1) and are shown in Fig. 4S. The flux results for the climatic types showed significant differences (Kruskal–Wallis test; $p < 0.5$; $\alpha = 0.05$) between the different climatic types of the study region; it seems evident that the *Am* and *BSh* types exports more inorganic (DIC + PIC) and organic (DOC + POC) carbon (Fig. 4Sa, Sb, and Sc). The inorganic form showed higher fluxes compared to the organic forms. Type *Am* had an average flux of 88.0 ± 80 g C m^{-2} yr^{-1}; whereas climate type *BSh* had a flux of 42.0 ± 10 g C m^{-2} yr^{-1} (Fig. 4Sa). DIC fluxes accounted for > 90% of inorganic forms in the *Am* and *BSh* climate types. For organic forms, DOC fluxes represented the highest percentages in climate types *Am* (70%) and *BSh* (74%).

About N fluxes, Fig. 4S shows the *Am* and *BSh* climate types with higher rates. The *Am* type prevails over the *BSh* type with a 2.3 times higher rate (Fig. 4Sd). Inorganic nitrogen fluxes (average $= 2.5 \pm 11$ g N m^{-2} yr^{-1}) represent almost twice the organic nitrogen fluxes (average $= 1.3 \pm 5$ g N m^{-2} yr^{-1}). The organic/inorganic ratio was estimated at O/I = 0.6 for all climate types (Fig. 4Se and Sf). The main organic influence is the *As* type (O/I = 0.64) and the main inorganic influence is the *Am* type (I/O = 0.5).

P fluxes were higher in the *Am*, *BSh,* and *Af* climate types, respectively (Fig. 4Sg). The mean inorganic P flux (0.06 ± 0.2 g P m^{-2} yr^{-1}) was slightly higher than the organic P flux (0.04 g P m^{-2} yr^{-1}), respectively (Fig. 4Sh and Si). The ratio of organic/inorganic forms was O/I = 0.75; it was observed that in the *Am* and *As* types these ratios are slightly higher, indicating greater organic influence.

3.6 C-N-P Stoichiometry

Table 3 shows the percentages of the main constituents and their average stoichiometric ratios for the sixty rivers studied.

Using the conceptual ternary diagram, we plot the stoichiometric C/N/P ratios for all studied rivers (Fig. 5a). The results showed P depletion relative to C and/or N in 39 of the sixty rivers (65%) indicated in the ternary diagram (20–80%), 17 rivers indicated P and/or N depletion relative to C, three rivers showed a balance between C, N, and P (central sector of the diagram), and one river (ITM) with C and P co-depleted. These results show an excess of C and N relative to P. This was further supported by the fact that most catchments had TOC values > 50% (Table 3; Fig. 5a).

Here, we only include DIN and DIP as Nr, and Pr due to the lack of monitoring data for organic N and P fractions. However, our conclusions on the dominance of TOC, Nr not change, even in a scenario with high concentrations of TOC and reactive N (Table 3).

Stoichiometric ratios were also analyzed according to land use in the study region (Fig. 5b). The results showed P depletion in most monitoring stations (83%) of the sixty rivers (133 stations). Agricultural activity, savannah features and the urban area spatially dominate the study region associated with P depletion (Fig. 5b). The spatial patterns of the classes suggest that watershed landscape features exert a first-order control on average C/N/P reactive rates. Natural features also show P depletion; however, they can also be associated with N depletion. Anthropogenic influence through population density was included in the stoichiometric analysis (Fig. 5c), indicating P depletion in regions with low and high population density. Low population densities spread across the diagram; whereas high population densities remain in the region of depleted P and N (see Fig. 5c; 20–80% Nr and 0–20% Nr respectively).

The mean ratios shown in Table 3 indicated a mean value of N/P = 89:1 for all rivers in the study region, indicating the high loading of N relative to P.

Table 3 Mean stoichiometric constituents samples collected from sixty rivers refer to the period 2008–2018

River [code]	TOC (%)	DIN (%)	DIP (%)	C/P	C/N	N/P
Almada [ALM]	83	13	4	1994	42	48
Colonia [COL]	58	29	13	474	13	36
Cachoeira [RCH]	62	20	18	363	21	18
Salgado [SLD]	76	18	6	1453	28	52
Salomé [SLM]	62	32	7	1005	13	78
Una [UNA]	62	32	6	1049	13	80
Tijuípe [TIJ]	63	30	7	1033	14	74
Das Almas [DAL]	75	21	3	2455	23	106
Baiano [BAI]	55	39	7	861	9	92
Camarugi [CMG]	55	44	1	7176	8	861
Jaguaripe [JGP]	55	36	9	660	10	66
Jequiriçá mirim [JQM]	94	1	5	1808	817	2
Jequiriçá [JQM]	72	26	3	2750	18	149
Preto [P13]	52	43	5	1062	8	134
Carinhanha [CRN]	67	30	2	2921	15	197
Itaguari [IGR]	57	40	3	1950	9	210
Corrente [CRT]	63	33	4	1623	13	128
Formoso [FOM]	65	29	5	1324	15	90
Guará [GUA]	48	46	6	781	7	113
Do Antonio [ANT]	22	76	2	1292	2	686
Brumado [BRU]	58	38	5	1356	10	134
Contas [COM]	66	29	5	1334	15	89
Gavião [GAV]	86	1	13	722	560	1
Gongoji [GGI]	84	8	7	1214	69	18
Jequiezinho [JQZ]	32	41	27	127	5	24
Do Peixe [PEX]	55	42	3	1839	9	213
Das Femeas [FEM]	83	3	14	609	214	3
Grande [GRD]	67	30	3	2583	15	177
Preto [P11]	45	48	7	737	6	118
Branco [RBR]	77	12	11	720	42	17
De Janeiro [RJN]	83	5	12	720	115	6
De Ondas [RON]	52	40	8	657	9	77
Do Aipim [AIP]	54	42	4	1434	8	169
Itapicuru açu [ITA]	78	19	3	2583	27	95
Itapicuru [ITP]	69	26	5	1381	17	79
Peixe de baixo [RPB]	84	15	1	10,013	37	267
Itapicuru mirim [ITM]	17	80	3	630	1	439
Jequitinhonha [JQH]	68	28	5	1531	16	95
Jacuípe [JCP]	66	24	10	727	18	40
Paraguaçu [PRG]	82	15	3	2909	36	82
De Una [RDU]	94	3	3	3576	188	19
Utinga [UTG]	77	11	12	679	46	15
Catolé Grande [CGR]	35	45	21	179	5	35
Córrego Lagoa do Baixo [CLB]	67	31	1	5267	14	370
Pardo [PRD]	68	28	4	1616	16	100
Real [REA]	40	36	24	180	7	24

Table 3 (continued)

River [code]	TOC (%)	DIN (%)	DIP (%)	C/P	C/N	N/P
Salitre [SAL]	76	23	1	6847	22	305
Vaza-Barris [VZB]	73	23	4	2102	21	100
Buranhém [BRH]	73	22	5	1550	23	69
Dos Frades [FRD]	70	16	15	509	29	17
São Francisco [RSF]	67	29	3	2166	15	142
João de Tiba [JTB]	74	19	8	1008	26	39
Curaçá [CRC]	62	34	4	1735	12	144
Paramirim [PMI]	65	31	4	1628	14	116
Alcobaça [ALB]	75	21	4	2179	24	92
Jucuruçu Braço Norte [JUN]	54	40	7	871	9	98
Jucuruçu Braço Sul [JUS]	66	23	11	645	19	33
Peruípe do Sul [PRP]	95	1	4	2842	436	7
Jacaré [JRE]	91	5	4	2428	110	22
Verde [VRD]	73	24	3	2685	20	134

4 Discussion

The analysis of the data series obtained through the proposed methodology (time series: 10 years; frequency: bi-monthly) represented an important source of information for obtaining trends in C-N-P elements and also for identifying the current state of water quality in the 60 river systems. We believe that the geographical coverage of the systems analyzed represents a good distribution in the tropical region from the coast to the interior of the continent. This coverage includes 10º of latitude and 5 different climatic regions. Some limitations were identified (more frequent sampling, time series > 10 years) that could have provided more information; however, we believe that these results give us a good overview of trends and the current state of C-N-P concentrations and fluxes.

The analysis of the climatological series showed a well-defined pattern between the coastal and inland regions of the continent. Additionally, the trend analysis (Mann–Kendall test) showed no significant differences ($p > 0.05$) in rainfall in the study region for the 30-year period. These climate patterns from 2 different regions were also observed by Molion and Bernardo (2002) and Silva et al. (2012). Thus, we can suggest that the controlling factors of C-N-P variations are associated with anthropogenic origin, such as: agriculture, domestic and industrial sewage and livestock, mainly. According to Drake et al. (2021), Amazon River DOC concentrations ranged from 2.86 to 5.23 mg C l^{-1}, with a mean of 4.19 mg C l^{-1}; whereas in our study, DOC ranged from 4 to 21 mg C l^{-1}, with a mean value of 7.6 mg C l^{-1}. For DIN, Drake et al. (2021), reported a range of 0.08—0.28 mg N l^{-1}; whereas the DIN in our study corresponded to a much larger range (0.02 to 15.8 mg N l^{-1}). The DIP reported for the Amazon River (Drake et al., 2021), ranged from 0.006 to 0.02 mg l^{-1}; this range is lower than that observed in our study (0.002—1.1 mg P l^{-1}). The C-N-P concentrations of our study region have higher concentrations than those reported by Drake et al (2021) in the Amazon River. These high concentrations are significant and indicate a warning sign in the flux estimates for this study region.

To analyze the inputs of C-N-P exported by the sixty rivers to the coastal region we included the fluxes of these loads. The export of fluvial C from land to the ocean is an important interface between two of the largest carbon reservoirs in the world. Recent syntheses have provided revised estimates for the riverine transport of C that river water annually provides 0.80—1.33 Pg of C to the world's oceans (Huang et al., 2012), in which organic carbon (TOC) accounts for about 45% (Cai, 2011; Meybeck, 1982). In the tropical region (30ºN – 30ºS), the fluvial input of C delivers approximately 0.53 Pg carbon to the estuaries annually. Of this, 0.21 Pg C is dissolved inorganic carbon (DIC), 0.14 Pg C is dissolved

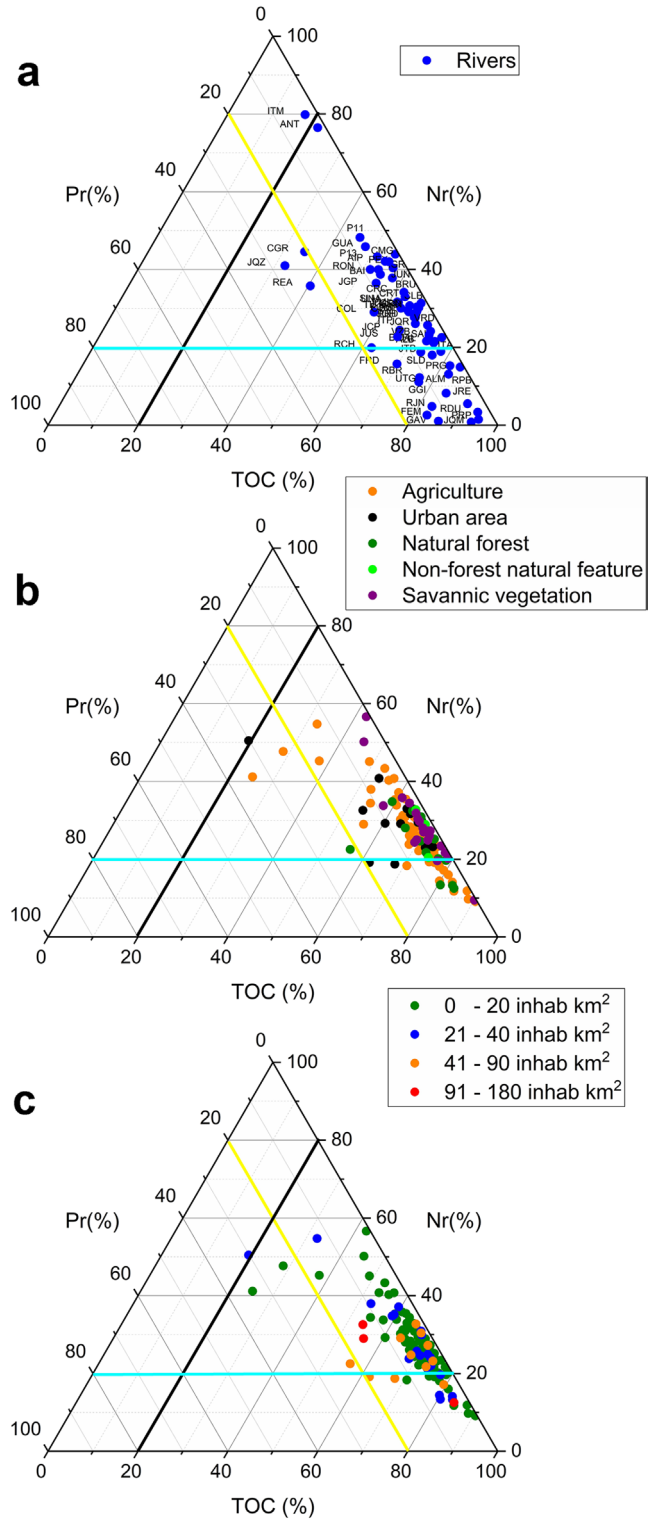

Fig. 5 Classification of different classes in ternary plot. According to Smith et al. (2017); (i) values in the central portion of the graph would be "balanced" relative to each other; (ii) values to the right of the yellow line would be P depleted (i.e., < 20% TDPR); (iii) values to the left of the black line would be C depleted (i.e., < 20% TOC); and (iv) values below the cyan line would be N depleted (i.e., < 20% TDNR). The corners would represent codepletion. Values with a "balanced" Redfield ratio (i.e., 106 C/16 N/1 P) would appear at the coordinates 33.3% TDC, 33.3% TDNR, and 33.3% TDPR; **a** Stoichiometric ratios of C-N-P at all rivers; **b** stoichiometric ratios at all stations in hydrographic basins categorized according to land-use; and (**c**) stoichiometric ratios at all stations categorized according to population density

organic carbon (DOC), 0.05 Pg C is particulate inorganic carbon (PIC), and 0.13 Pg C is particulate organic carbon (POC) (Huang et al., 2012).

Global annual export of total N (TN), P (TP) and organic C (TOC) from rivers is estimated to be 44.9 Tg N, 9.04 Tg P, and 317 Tg C respectively.

Estimates of the C fluxes (Tg yr^{-1}) of the studied rivers are shown in Fig. 3a indicated the annual total C load (TC) of 32.7 Tg C yr^{-1} (0.0327 Pg C yr^{-1}), where DIC accounted for 69% of TC (22.7 Tg C yr-1), and DOC contributed 22% (6.9 Tg C yr^{-1}). According to our results, the DOC represented ~ 27% of DOC export by Amazon River (average = 25.0 Tg C yr^{-1}; Moreira-Turcq et al., 2003; Huang et al., 2012; Drake et al., 2021). When compared to tropical rivers in the Americas (Huang et al., 2012), exported DOC represented approximately 12% of the total.

Estimated total N (TN) loads amounted to 1.6 Tg N yr^{-1} (Fig. 3b), where DIN represented 44% of TN (0.7 Tg N yr^{-1}). This flux is like that reported by Drake et al. (2021) in the Amazon River (0,82 Tg DIN yr^{-1}). According to Mayorga et al. (2010), modeled N fluxes for South American rivers represent ~ 8.0 Tg N yr^{-1}. These authors also indicate DIN fluxes between 40—570 kg km^{-2} yr^{-1} for the study region, whereas our fluxes indicated a mean value of 196 kg km^{-2} yr^{-1}.

P loads amounted to 0.07 Tg P yr-1 (Fig. 3c); where DIP accounted for 29% of the TP (0.02 Tg P yr^{-1}). This DIP load is approximately one third of the load reported by Drake et al. (2021) for the Amazon River (0.063 Tg P yr^{-1}). Modeled yearly fluxes of DIP were reported by Mayorga et al. (2010), indicating a range of 2–5 kg km^{-2} yr^{-1}; whereas our study indicated a mean value of 7.9 kg km^{-2} yr^{-1}.

A temporal analysis of these fluxes between 2008—2018 showed a significant increasing trend for TOC (Fig. 4b). According to Mayorga et al. (2010), yearly DOC fluxes range between 250—4000 kg C km^{-2} yr^{-1} for the study region, whereas the observed range of DOC varied between 12—3300 kg C km^{-2} yr^{-1}. The slope of this series indicated an increase of 0.001 g C m^{-2} yr^{-1} for the TOC time series (Fig. 4b). This rate is indicative of the fact that the values observed in this study increase in accordance with the growth and expansion of urban and agricultural areas.

We analyzed the produced and remaining organic loads (that which reaches the receptor aquatic body) for the 2008–2018 series of all municipalities ($N = 417$). Trend analysis (Mann–Kendall test; $\alpha = 0.05$) showed 85% of municipalities ($N = 354$) with a positive trend ($p < 0.05$) and 63 municipalities with a negative remaining organic load (15%). These results are also associated with the population density observed for the study period (Fig. 6a).

The high rate of positive trends in the remaining organic load is indicative of urban and agricultural expansion in the region (Fig. 6b). The organic load entering the rivers is increasing progressively, mainly due to poor public sanitation policies. In the study region only 19 municipalities have a remaining organic load of < 40% (acceptable % of discharge into the water body); this represents < 5% of the municipalities in the region ($N = 417$).

Land use and cover were analyzed for the period 2008–2018 (Fig. 6b, c and d). The results indicated a trend of increasing anthropized area of 4% for this period, whereas the natural area decreased by 3.1% for the same period. As observed in Fig. 6a, the average C load represents approximately 15 times the load of natural origin (30.7×10^6 t yr^{-1}). Similar flux increases can also be observed for N and P respectively. In this sense, we should consider the C-N-P stoichiometry that also indicated a P depletion; thus, the high organic load (positive TOC trend) reflects the urban and agricultural expansion in most municipalities and rivers of the region. The C-N-P loads reported here represent an important contribution to the regional and global balance of these macronutrients in tropical rivers.

4.1 Implications for Freshwater Management

The results of the study presented, which analyzed the relationships between the elements carbon (C), nitrogen (N) and phosphorus (P) in tropical river ecosystems, have significant implications for freshwater management and conservation efforts in these areas. In this analysis, we will explore the main implications of each element and propose actions for different sectors.

4.1.1 Implications of Carbon (C)

C Cycle C dynamics in tropical rivers are complex and influenced by various factors, such as vegetation, microbial activity and sedimentation. Changes in the C cycle can affect water quality, primary productivity and the structure of aquatic communities.

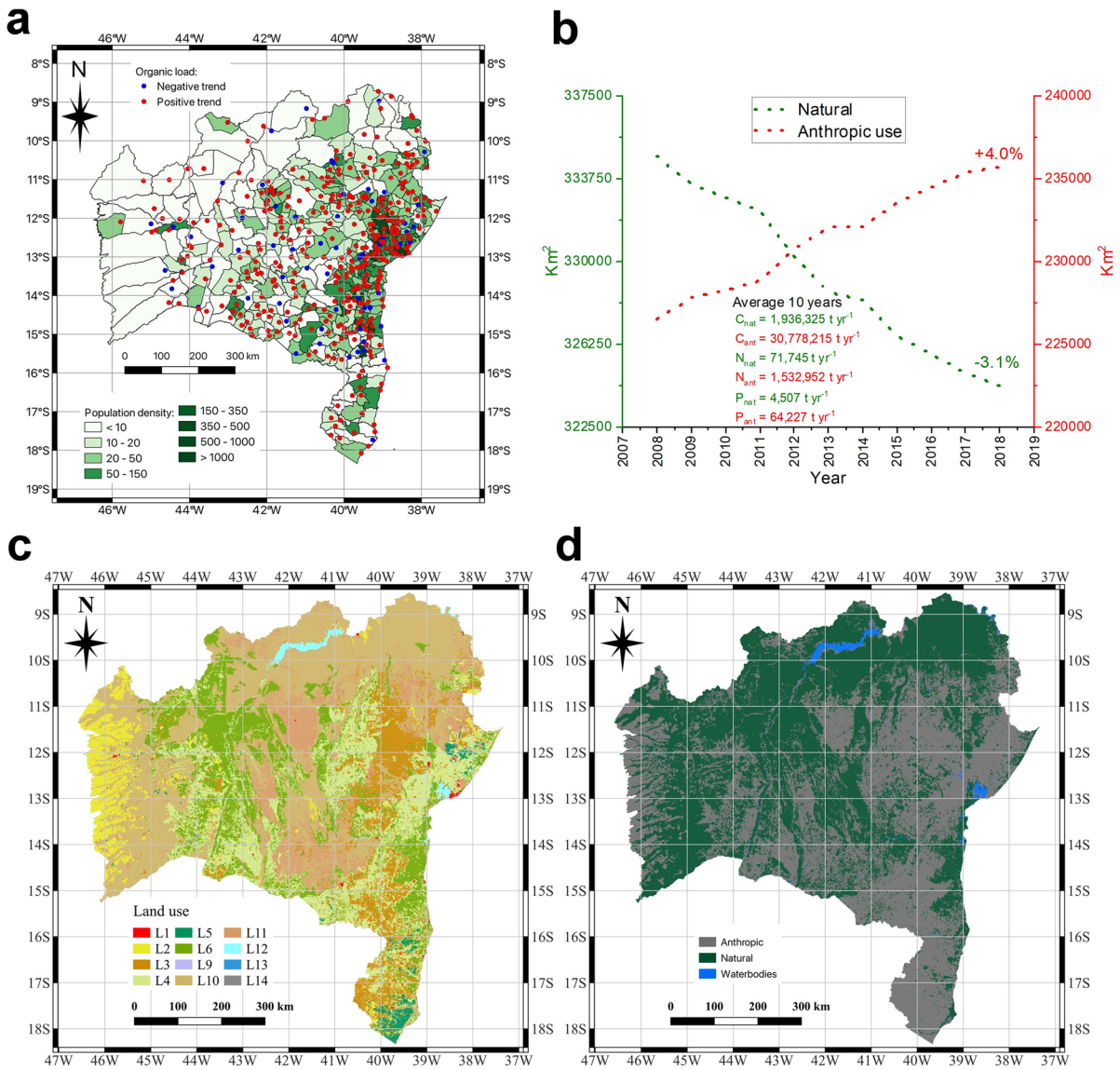

Fig. 6 Trends of organic load in 417 municipalities of the study region (**a**); variations of anthropogenic (km^2) and natural (km^2) expansion (**b**); categorized distribution of land-use in the study region (**c**); and distribution of anthropic and natural areas (**d**). L1 = Artificial area; L2 = Agricultural area; L3 = Managed Pasture; L4 = Mosaic of occupations in forest area; L5 = Silviculture; L6 = Forest vegetation; L7 = Wetland; L8 = Grassland vegetation; L9 = Mosaic of occupations in grassland area; L10 = Continental water body; L11 = Coastal water body and L12 = Uncovered area

Greenhouse Gas Emissions Tropical rivers can be significant sources of greenhouse gases such as carbon dioxide (CO_2) and methane (CH_4). Inadequate water and soil management can increase greenhouse gas emissions, exacerbating climate change.

Carbon Sequestration Tropical rivers can also act as carbon sinks, storing carbon in sediments and plant biomass. The protection and sustainable management of river ecosystems can contribute to mitigating climate change.

4.1.2 Implications of Nitrogen (N)

Eutrophication N excess in rivers can lead to eutrophication, a process that causes excessive algae growth and reduced oxygenation of the water. Eutrophication can have negative impacts on water quality, aquatic fauna and flora and human use of water.

Nitrate Pollution Nitrate, a form of N, can contaminate groundwater and represent a risk to human health. Appropriate fertilizer and wastewater management is crucial to prevent nitrate pollution.

N Cycling N is an essential element for life and plays an important role in the primary productivity of aquatic ecosystems. Understanding the N cycle is fundamental to the sustainable management of water resources.

4.1.3 Implications of Phosphorus (P)

Nutrient Limitation P is often a limiting nutrient in tropical rivers, meaning that its availability controls the growth of algae and other aquatic plants. Changes in P levels can affect the structure of aquatic communities and primary productivity.

P Pollution P excess in rivers can lead to eutrophication, with the same negative consequences as those mentioned above for N. Proper management of fertilizers, detergents and sewage is essential to prevent P pollution.

Bioavailability of P The form and bioavailability of phosphorus in rivers are important for the assimilation of this element by aquatic organisms. Understanding these aspects is crucial for the sustainable management of water resources.

4.2 Actions for freshwater management and conservation

Implementation of integrated water resources management policies: Policies should consider the biogeochemical cycles of C, N and P and promote the sustainable use of water.

Improving Water Quality Monitoring Collecting and analyzing data on C, N and P levels in rivers is essential for understanding the dynamics of these elements and identifying potential problems.

Restoring Riparian Areas Restoring degraded areas along rivers can help filter nutrients and reduce water pollution.

Developing Sustainable Agricultural Practices Practices such as agroecology can help reduce the use of fertilizers and soil erosion, reducing the amount of nutrients entering rivers.

Promoting Environmental Education Raising awareness about the importance of fresh water and the challenges of managing it is fundamental to changing behavior and adopting sustainable practices.

Scientific Research More research is needed to better understand the biogeochemical cycles of C, N and P in tropical rivers and to develop effective solutions for freshwater management and biodiversity conservation.

5 Conclusions

The results obtained from the time series of hydrochemical and demographic variables in 60 tropical rivers showed that the potential impact of anthropogenic activities over a decade on freshwater bodies. The trend analysis showed no significant differences in rainfall in the study region for the 30-year period. Thus, we can suggest that the controlling factors of C-N-P variations are associated with anthropogenic origin, such as: agriculture, domestic and industrial sewage and livestock, mainly.

The annual total C load (TC) was estimated at 32.7 Tg C yr^{-1}, where DIC accounted for 69% of TC and DOC contributed 22%. When compared to tropical rivers in the Americas, exported DOC represented approximately 12% of the total.

The inorganic forms of DIN and DIP represented the main components of TN and TP, respectively. DIN fluxes were like other tropical rivers (196 kg km^{-2} yr^{-1}), while TP showed higher fluxes than those reported by other studies for tropical areas.

The stoichiometry showed P depletion relative to C and/or N in 39 of the sixty rivers (65%). This was further supported by the fact that most catchments had TOC values > 50% (C/N/P = 100%). A significant trend was found for TOC.

Land-use and cover at period 2008–2018 indicated a trend of increasing anthropized area of 4%, whereas the natural area decreased by 3.1%. The organic load trend analysis showed 85% of cities with a positive trend, this high rate in the remaining organic load is indicative of urban and agricultural in the region.

The results obtained for the C-N-P elements in this study contributed to characterizing the current state of water quality in 60 rivers, their fluxes, and their trends. This has generated important information that can be used in the future studies at other authors aimed at complementing time series and their associations with anthropogenic factors.

Acknowledgements The authors would like to thank INEMA (Instituto do Meio Ambiente e Recursos Hídricos) for the availability of hydrochemical data. C. N. was supported by FADE (Fundação de Apoio ao desenvolvimento da UFPE) contract Nº04/2018 under grant agreement Nº 5850.0108524.18.9. H. L. V. acknowledges the TRIATLAS project, which has received funding from the European Union's Horizon 2020 Research and Innovation Program under grant agreement no 817578 and the International Joint Laboratory TAPIOCA (IRD-UFPE-UFRPE).

Author Contributions Carlos Noriega: Conceptualization, Methodology, Visualization, Software, Validation, Formal analysis, Writing – original draft, Writing – review & editing. Moacyr Araujo: Visualization, Supervision, Funding acquisition, Writing – original draft. Carmen Medeiros: Visualization, Writing – original draft, Funding acquisition. Humberto L. Varona: Conceptualization, Methodology, Software, Validation, Formal analysis, Visualization, Writing – original draft, Writing – review & editing. Aubains Hounsou-Gbo: Software, Visualization, Formal analysis, Writing – original draft. Julia Araujo: Visualization, Writing – original draft.

Data Availability The authors declare that the data supporting the findings of this study are available at http://www.inema.ba.gov.br/servicos/monitoramento/qualidade-das-aguas/ or on request.

Declarations

Competing Interest The authors declare that they have no known competing financial interests or personal relationships that could have appeared to influence the work reported in this paper.

References

APHA. (2005). *Standard Methods for the Examination of Water and Wastewater* (21st ed.). American Public Health Association/American Water Works Association/Water Environment Federation.

Bauer, J. E., Wei-Jun, C., Raymond, P. A., Bianchi, T. S., Hopkinson, C. S., & Regnier, P. A. (2013). The changing carbon cycle of the coastal ocean. *Nature, 504*, 61. https://doi.org/10.1038/nature12857

Blaen, P. J., Khamis, K., Lloyd, C., Comer-Warner, S., Ciocca, F., Thomas, R. M., MacKenzie, A. R., & Krause, S. (2017). High-frequency monitoring of catchment nutrient exports reveals highly variable storm event responses and dynamic source zone activation. *Journal of Geophysical Research. Biogeosciences, 122*(9), 2265–2281. https://doi.org/10.1002/2017JG003904

Cai, W.-J. (2011). Estuarine and Coastal Ocean Carbon Paradox: CO_2 Sinks or Sites of Terrestrial Carbon Incineration? *Annual Review of Marine Science, 3*, 123–145. https://doi.org/10.1146/annurev-marine-120709-142723

Causse, J., Baurés, E., Mery, Y., Yung, V. A., & Thomas, O. (2015). Variability of N export in wáter: A review. *Environmental Sciences, 45*(20), 2245–2284. https://doi.org/10.1080/10643389.2015.1010432

Drake, T. W., Hemingway, J., Kurek, M. R., Peucker-Ehrenbrink, B., Brown, K., Holmes, R., Galy, V., Moura, J. M., Mitsuya, M., Six, J., & Spencer, R. G. M. (2021). The pulse of the Amazon: fluxes of dissolved organic carbon, nutrients, and ions from the world's largest river. *Global Biogeochemical Cycles, 35*, e2020GB006895. https://doi.org/10.1029/2020GB006895

Eyre, B., & Ferguson, A. (2002). Comparison of carbon production and decomposition, benthic nutrient fluxes and denitrification in seagrass, phytoplankton, benthic microalgae- and macroalgae-dominated warm-temperate Australian lagoons. *Marine Ecology Progress Series, 229*, 43–59. https://doi.org/10.3354/meps229043

Gruber N, Galloway J (2008). An Earth-system perspective of the global nitrogen cycle. *Nature*. 451/293–296. https://doi.org/10.1038/nature06592

Huang, T.-H., Fu, Y.-H., Pan, P.-Y., & Chen, C. T. A. (2012). Fluvial carbon fluxes in tropical rivers. *Current Opinion in Environment Sustainability, 4*, 162–169. https://doi.org/10.1016/j.cosust.2012.02.004

Instituto Brasileiro de Geografia e Estatística - IBGE (2010). Censo Demográfico. Retrieved March 1, 2023, from https://www.ibge.gov.br/estatisticas/sociais/populacao/9662-censo-demografico-2010html?edicao=9673&t=resultados. (in portuguese).

Instituto Brasileiro de Geografia e Estatística - IBGE (2021). Areas Territoriais. Retrieved March 1, 2023, from https://www.ibge.gov.br/geociencias/organizacao-do-territorio/estrutura-territorial/15761-areas-dos-municipios.html?edicao=33086&t=acesso-ao-produto. (in portugues).

Instituto do meio Ambiente e Recursos Hidricos – INEMA (2018). Monitoramento e qualidade das águas. http://

www.inema.ba.gov.br/servicos/monitoramento/qualidade-das-aguas/. Accessed in Oct 2023.

Instituto Nacional de Meteorologia-INMET (2018). Banco de dados meteorologicos. https://portal.inmet.gov.br/. Accessed in Oct 2023.

Islam, M. J., Jang, C., Eum, J., Jung, S. M., Shin, M. S., Lee, Y., Choi, Y., & Kim, B. (2019). C:N: P stoichiometry of particulate and dissolved organic matter in river waters and changes during decomposition. *Journal of Ecology and Environment, 43*, 4. https://doi.org/10.1186/s41610-018-0101-4

Jani, J., & Toor, G. (2018). Composition, sources, and bioavailability of nitrogen in a longitudinal gradient from freshwater to estuarine waters. *Water Research, 137*, 344–354. https://doi.org/10.1016/j.watres.2018.02.042

Jarvie, H. P., Smith, D. R., Norton, L. R., Edwards, F. K., Bowes, M. J., & Bachiller-Jareno, N. (2018). Phosphorus and nitrogen limitation and impairment of headwater streams relative to rivers in Great Britain: A national perspective on eutrophication. *Science of the Total Environment, 621*, 849–862. https://doi.org/10.1016/j.scitotenv.2017.11.128

Jeanneau, L., Richard, R., & Shreeram, I. (2018). Molecular fingerprinting of particulate organic matter as a new tool for its apportionment: Changes along a headwater drainage in coarse, medium and fine particles as a function of rainfalls. *Biogeosciences, 5*(4), 973–985. https://doi.org/10.5194/bg-15-973-2018

Liu, Q., Liang, Y., Cai, W.-J., Wang, K., Wang, J., & Yin, K. (2020). Changing riverine organic C:N ratios along the Pearl River: Implications for estuarine and coastal carbon cycles. *Science of the Total Environment, 709*. https://doi.org/10.1016/j.scitotenv.2019.136052

Mayorga, E., Seitzinger, S., Harrison, J., Dumont, E., Beusen, A., Bouwmand, A. F., Fekete, B., Kroeze, C., & Van Drecht, G. (2010). Global Nutrient Export from WaterSheds 2 (NEWS 2): Model development and implementation. *Environmental Modelling and Software, 25*, 837–853. https://doi.org/10.1016/j.envsoft.2010.01.007

Meybeck, M. (1982). Carbon, nitrogen, and phosphorus transport by World Rivers. *American Journal of Science, 282*, 401–450.

Molion L, Bernardo S (2002). Uma revisão da dinâmica das chuvas no nordeste brasileiro. *Revista Brasileira de Meteorologia 17*(1), 1–10. https://www.scielo.br/j/rbmet/grid. Accessed 27 Oct 2023.

Moreira-Turcq, P., Seyler, P., Guyot, J. L., & Etcheber, H. (2003). Exportation of organic carbon from the Amazon River and its main tributaries. *Hydrological Processes, 17*(7), 1329–1344. https://doi.org/10.1002/hyp.1287

National Meteorological Institute-INMET (2023). Meteorological Database for Teaching and Research – BDMEP. https://bdmep.inmet.gov.br/. Accessed 01 Apr 2023

Noriega, C., & Araujo, M. (2014). Carbon dioxide emissions from estuaries of northern and northeastern Brazil. *Scientific Reports, 4*, 6164. https://doi.org/10.1038/srep06164

Peacock, M., Futter, M., Jutterström, S., Kothawala, D., Moldan, F., Stadmark, J., & Evans, C. (2022). Three Decades of Changing Nutrient Stoichiometry from Source to Sea on the Swedish West Coast. *Ecosystems, 25*, 1809–1824. https://doi.org/10.1007/s10021-022-00798-x

Santos, H. G., Jacomine, P. K., Anjos, L. H., Oliveira, V. A., Lumbreras, J. F., & Coelho, M. R. (2018). *Sistema brasileiro de classificação de solos* (5th ed.). Brasilia.

Silva, C. P., Souza Filho F., & Lázaro, Y. (2012). Sazonalidade da Precipitação Sobre o Nordeste Setentrional Brasileiro nas Simulações do IPCC-AR4. *Revista Brasileira de Recursos Hídricos, 17*(3), 125–134. https://www.scielo.br/j/rbrh/grid. Accessed 25 Oct 2023.

Smith, D. R., Jarvie, H. P., & Bowes, M. J. (2017). Carbon, nitrogen, and phosphorus stoichiometry and eutrophication in river thames tributaries, UK. *Agricultural & Environmental Letters, 2*, 170020. https://doi.org/10.2134/ael2017.06.0020

Stutter, M. I., Graeber, D., Evans, C. D., Wade, A. J., & Withers, P. J. A. (2018). Balancing macronutrient stoichiometry to alleviate eutrophication. *Science of the Total Environment, 634*, 439–447. https://doi.org/10.1016/j.scitotenv.2018.03.298

Tanioka, T., Garcia, C., Larkin, A., Garcia, N., Fagan, A., & Martiny, A. (2022). Global patterns and predictors of C:N:P in marine ecosystems. *Communication Earth & Environment, 3*, 271. https://doi.org/10.1038/s43247-022-00603-6

Varona, H. L., Noriega, C., Araujo, J., Lira, S., Araujo, M., & Hernandez, F. (2023). mStatGraph: Exploration and statistical treatment software to process, compute and validate oceanographic data. *Software Impacts, 17*, 100571. https://doi.org/10.1016/j.rsma.2023.103071

Wachholz, A., Dehaspe, J., Ebeling, P., Kumar, R., Musolff, A., Saavedra, F., Winter, C., Yang, S., & Graeber, D. (2023). Stoichiometry on the edge - humans induce strong imbalances of reactive C:N: P ratios in streams. *Environmental Research Letters, 18*, 044016. https://doi.org/10.1088/1748-9326/acc3b1